AD_____

Award Number: W81XWH-08-2-0067

TITLE: Small Molecule Activators of the TRK Receptors for Neuroprotection

PRINCIPAL INVESTIGATOR: Nicholas J. Webster, Ph.D. Small Molecule Activators of the TRK Receptors for Neuroprotection

CONTRACTING ORGANIZATION: Veterans Medical Research Foundation
San Diego, CA 92161-0002

REPORT DATE: May 2011

TYPE OF REPORT: Final

PREPARED FOR: U.S. Army Medical Research and Materiel Command
Fort Detrick, Maryland 21702-5012

DISTRIBUTION STATEMENT: Approved for Public Release;
Distribution Unlimited

REPORT DOCUMENTATION PAGE

Form Approved
OMB No. 0704-0188

1. REPORT DATE	2. REPORT TYPE	3. DATES COVERED
1 May 2011	Final	1 MAY 2008 - 30 APR 2011

4. TITLE AND SUBTITLE

Small Molecule Activators of the TRK Receptors for Neuroprotection

5a. CONTRACT NUMBER

5b. GRANT NUMBER
W81XWH-08-2-0067

5c. PROGRAM ELEMENT NUMBER

6. AUTHOR(S)
Nicholas J. Webster, Ph.D., Stan Krajewski, M.D., Ph.D., and
Michael C. Pirrung, Ph.D.

E-Mail: nwebster@ucsd.edu

5d. PROJECT NUMBER

5e. TASK NUMBER

5f. WORK UNIT NUMBER

7. PERFORMING ORGANIZATION NAME(S) AND ADDRESS(ES)

Veterans Medical Research Foundation
San Diego, CA 92161-0002

8. PERFORMING ORGANIZATION REPORT NUMBER

9. SPONSORING / MONITORING AGENCY NAME(S) AND ADDRESS(ES)
U.S. Army Medical Research and Materiel Command
Fort Detrick, Maryland 21702-5012

10. SPONSOR/MONITOR'S ACRONYM(S)

11. SPONSOR/MONITOR'S REPORT NUMBER(S)

12. DISTRIBUTION / AVAILABILITY STATEMENT
Approved for Public Release; Distribution Unlimited

13. SUPPLEMENTARY NOTES

14. ABSTRACT
Our central hypothesis is that asterriquinone activators of the Trk receptors would prevent the neuronal cell death associated with traumatic brain injury and would improve cognitive and motor outcomes. We have developed agonists to TrkA and TrkB. The TrkA agonist has been tested in a preclinical model of cognitive impairment and a model of traumatic brain injury. The drug improves learning in a Morris water maze paradigm and reduces infarct volume in a controlled cortical impact model of brain injury. Preliminary pharmacokinetic data indicates the drug is orally available. Further analogs with improve potency and specificity are being developed.

15. SUBJECT TERMS
indole, quinone, fluorinated, nerve growth factor, brain injury

16. SECURITY CLASSIFICATION OF:			17. LIMITATION OF ABSTRACT	18. NUMBER OF PAGES	19a. NAME OF RESPONSIBLE PERSON
a. REPORT	b. ABSTRACT	c. THIS PAGE			USAMRMC
U	U	U	UU		19b. TELEPHONE NUMBER *(include area code)*

Table of Contents

Introduction

The goal of this research program is to facilitate the discovery, development and clinical evaluation of effective therapies for traumatic brain injury with emphasis on the development of lead compounds through preclinical *in-vitro* and *in-vivo* evaluation, and the conduct of pre-clinical "proof of concept" studies. Our central hypothesis is that asterriquinone activators of the Trk receptors would prevent the neuronal cell death associated with traumatic brain injury and would improve cognitive and motor outcomes. We propose to develop agonists to TrkA, TrkB and TrkC. These agonists will be tested in preclinical models of Alzheimers neurodegeneration, as an extension of our current program, and into models of traumatic brain injury with the hope of identifying lead drugs that can be taken into early trials in humans.

Body of Report

The Statement of Work in the original proposal identified the following tasks.

Task 1: *Screen combinatorial library of asterriquinone and monoquinone compounds against the BDNF receptor TrkB and the neurotrophin 3 receptor TrkC.*

We have completed the screen against TrkB. The library of 334 asteriquinones and 62 monoquinones were tested for their ability to activate the TrkB using an ELISA assay that detects phosphorylated TrkB. Briefly, all tyrosine-phosphorylated proteins were captured by PY20 antibody coated on microtiter plates. The presence of TrkB among the phosphorylated proteins was then detected by anti-TrkB antibodies. Activation of TrkB was compared to stimulation by a maximal concentration of BDNF (100 ng/ml). In this assay, the original compound DAQ-B1 did not activate TrkB and our lead drug 5E5 activated to 74% the effect of BDNF. This is a little higher than the activation we measured by immunoblotting whole cell extracts (~40%) but may simply reflect the difference between the ELISA and western blot (1). Thirty-nine compounds had activity >25% BDNF.

We have completed the screen against TrkC. The library of 334 asteriquinones were

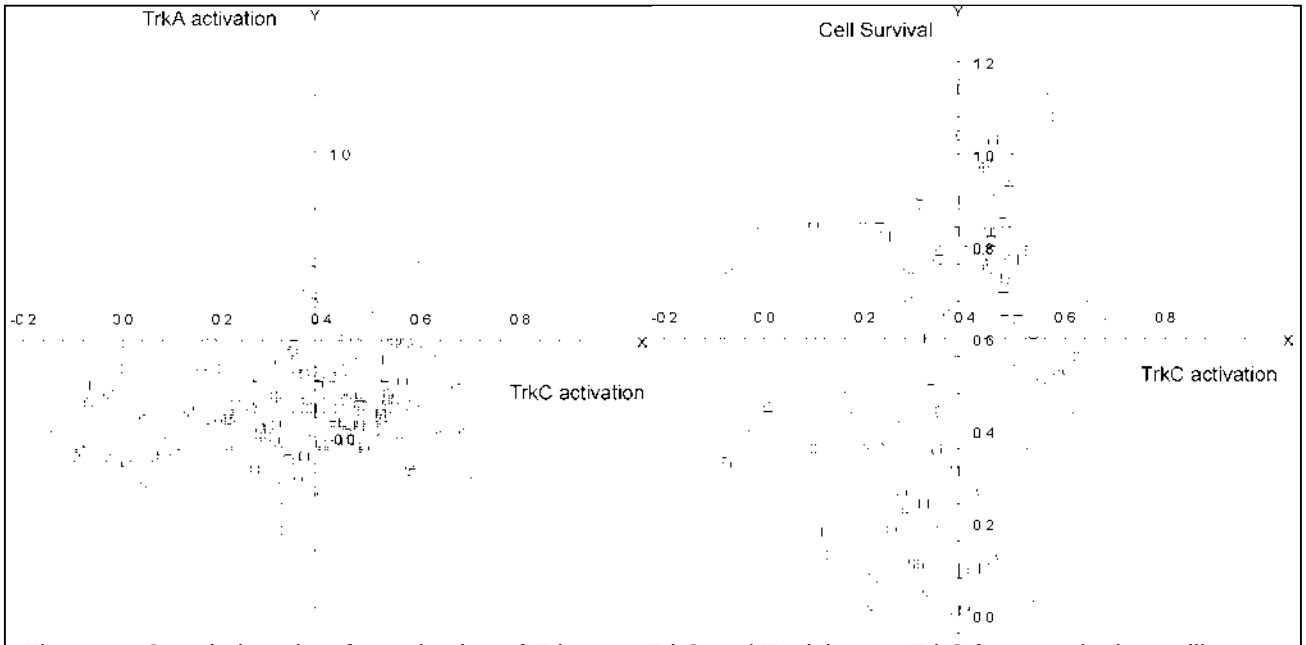

Figure 1: Correlation plots for activation of TrkA v.s. TrkC and Toxicity v.s. TrkC for asterriquinone library.

tested for their ability to activate the TrkC using an ELISA assay that detects phosphorylated TrkC. Briefly, all tyrosine-phosphorylated proteins were captured by PY20 antibody coated on microtiter plates. The presence of TrkC among the phosphorylated proteins was then detected by anti-TrkC antibodies. Activation of TrkC was compared to stimulation by a maximal concentration of NT3 (100 ng/ml). Activation of TrkC did not correlate with activation of TrkA or toxicity (Fig. 1) nor with activation of the insulin receptor (data not shown).

Task 2: *Model structure activity relationships for TrkB or TrkC activation using forward feed neural networks and multiple linear and nonlinear regression. Screen library of theoretical structures in silico using the derived models.*

We have modeled the activity of our compounds against TrkA, the insulin receptor, and for toxicity. The data for activity against the insulin receptor were generated under earlier funding from the American Diabetes Association but are included here in the modeling as a control for specificity. While not proposed in the original grant application, we felt that eliminating compounds that are insulin mimetics would help prevent any hypoglycemic complications.

We have modeled the activity of our compounds against TrkC using forward feed neural nets. Variability of substituent parameters was reduced by performing principal component analysis or by using Render nets. Neural nets were then generated using the top 50 components of the PCA or Render net analysis. The correlation of the PCA neural net modeled data with actual TrkC data is shown in Fig. 2. Similar results were obtained with Render reduced components. We compared the modeled activity data against previous datasets for TrkA and IR activation and toxicity (not shown). These additional data were included in the modeling as a control for specificity.

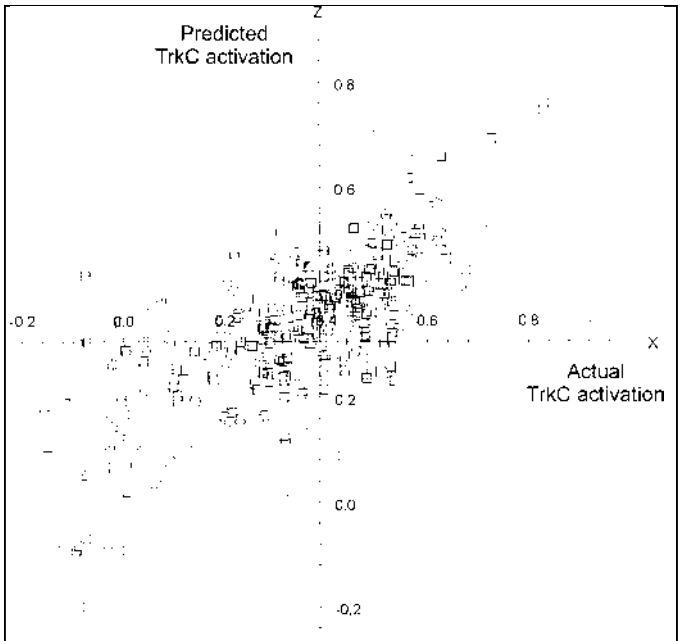

Figure 2: Mathematical modeling of TrkC activity. Plot shows correlation of activity predicted by PCA neural net model v.s. measured activity by ELISA.

Task 3: *Synthesize new asterriquinone and monoquinone compound libraries based on the mathematical modeling predictions.*

This project was focused on two main goals: the preparation of quantities of our lead compound, 5E5, sufficient to support animal studies; the preparation of fluorinated indoles and their conversion to 5E5 analogues. The scope of the work was a quite substantial amount of the 5E5 drug substance, in pure and crystalline form, and a half-dozen 5E5 analogues.

The synthesis of 5E5 is performed using a method earlier developed in our lab (2). It entails the acid-promoted condensation of 7-fluoroindole (**1**) with dichlorobenzoquinone, an *in situ* oxidation to give **2**, and then a solvolysis. Two methods have been used for the last step. The most direct is methanolysis, with hydroxide in methanol (Scheme 1). Sometimes, however, this reaction gives the dihydroxyquinone, which must then be methylated with dimethyl sulfate. Early work used the latter procedure to prepare about 1 g of 5E5. Later work was able to perform this conversion in a single step. We used this method to prepare our most recent sample of ca. 400 mg of 5E5. After chromatography, pure 5E5 was obtained that is a crystalline solid. Its recrystallization gives a highly pure sample of material that is very desirable for *in vivo* studies.

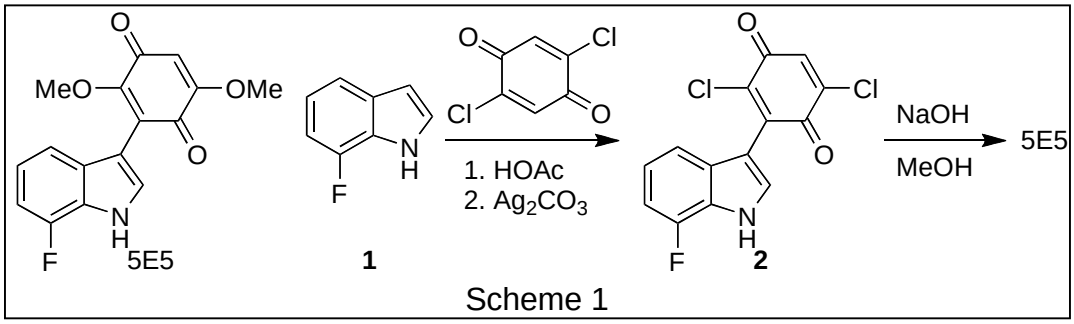

Scheme 1

Other indoles have been prepared for conversion to 5E5 analogues by one of two routes. Shown in Scheme 2 is the method applied to fluorinated anilines, which are commercially available. The amine is protected, which activates the adjacent CH bond for metalation and iodination. The resulting compound **4** is then coupled with a monoprotected acetylene using the Sonogashira reaction. Treatment with base removes its protecting group, causes closure of the heterocyclic ring, and deprotects the nitrogen, all in one step. The desired 6,7-difluoroindole (**5**) is the result. That compound could be subjected to the same route used to prepare 5E5 to access **6**.

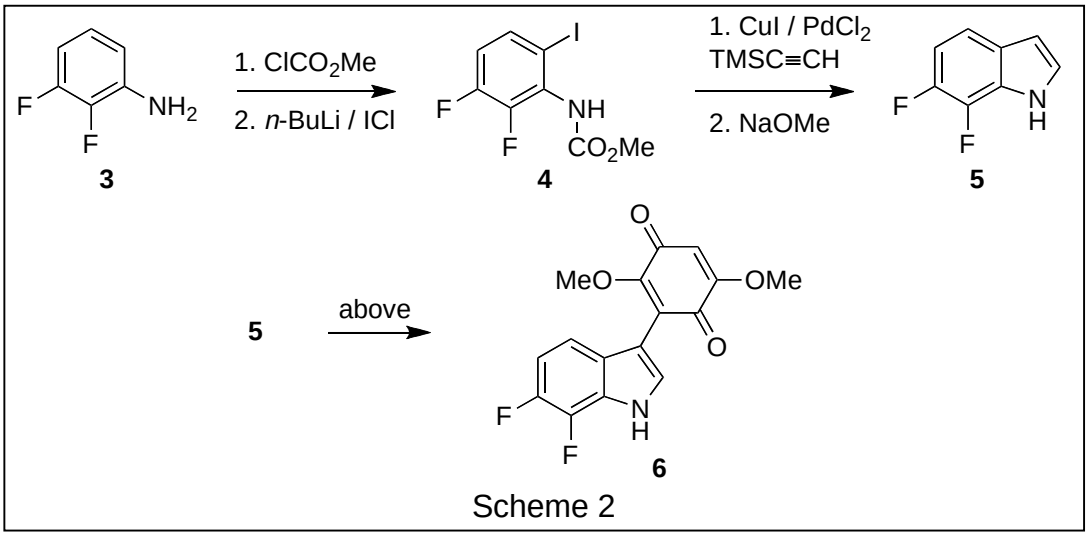

Scheme 2

Indoles **7**-**9** are also in hand (Scheme 3); the Sonogashira route was also used to prepare them from the corresponding anilines. For the remaining targeted indoles **10** and **11**, a different route was used. The Bartoli reaction is an excellent method to prepare indoles from nitrobenzenes (3), which are broadly available with a wide variety of substitution patterns. For example, the nitrobenzene precursors to **10** and **11** are available commercially or in a single step from a commercial material. Their Bartoli reactions are excellent processes to generate **10** and **11**.

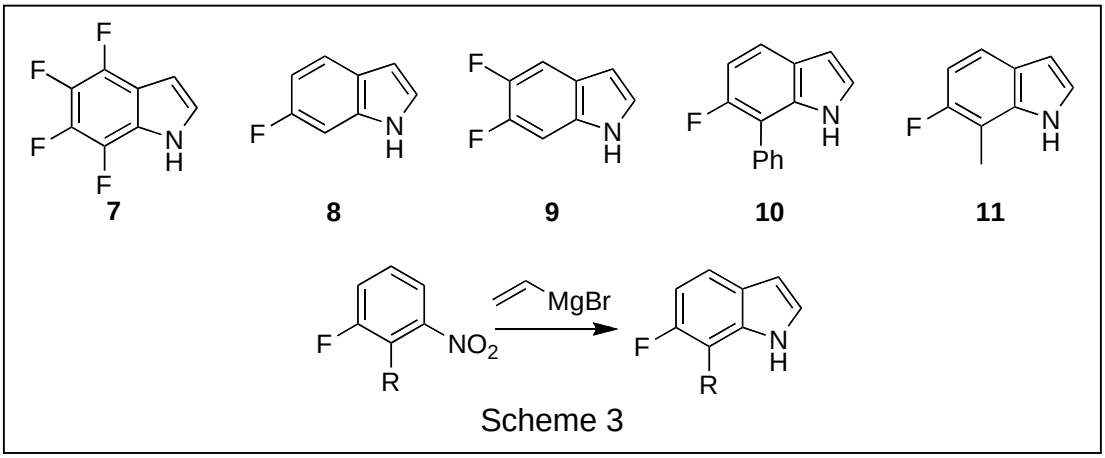

Scheme 3

We also focused on the preparation 5E5 analogues based on the design that came from earlier analyses in the Webster lab (Scheme 4). The indoles required are prepared using methods that we have detailed in earlier reports, and all were linked to the quinone unit using a standard set of reaction conditions we have also described earlier. The final products were prepared by treatment with basic methanol, purified to homogeneity, and their structures were established using NMR spectroscopy and high-resolution mass spectrometry. The total number of drug candidates that have been prepared here is 13, as depicted below, where in all cases the 'arrow' represents the connection to the common dimethoxy-benzoquinone substructure.

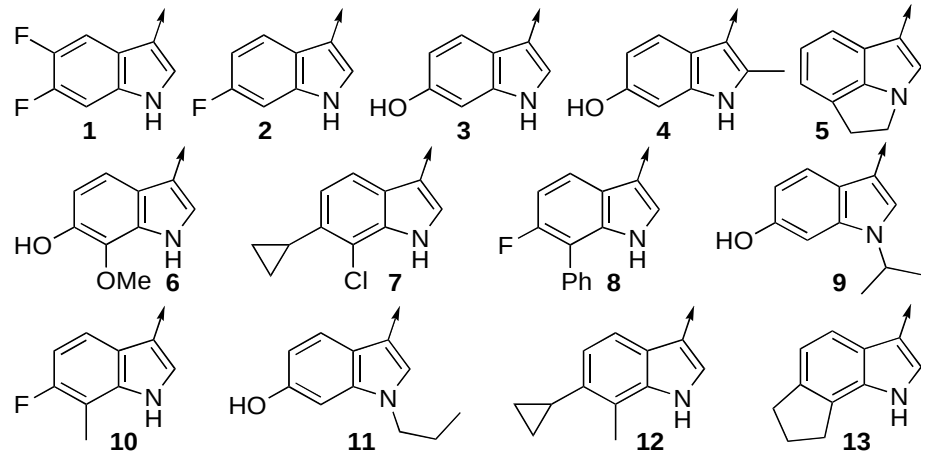

Scheme 4

Task 4: *Retest new compounds against TrkB and TrkC and for toxicity and refine mathematical models. Rerun in-silico predictions using theoretical library.*

New asteriquinones and monoquinones were tested against the Trk receptors and the data added to the mathematical models. The added data did significantly not improve the models as the r-squared values remain around 0.37.

Task 5: *Synthesize selected asterriquinone and monoquinone structures based on second round of predictions.*

This aim was not pursued as the models were not improved by the addition of new predicted analogs.

Task 6: *Test selected compounds for potency and selectivity for activation of Trk receptors. Test ability of compounds to support neuronal differentiation and neuronal survival using neuronal cells in culture.*

The original compound and a number of newer analogs were tested for selectivity against the Trk receptors. Testing of the in-vitro effects of these compounds is on going.

Task 7: *Test selected compounds for neuroprotective effects in a mouse model of neurodegeneration.*

We originally test our lead compound 5E5 in a reversal study in NGF+/- mice. We had previously shown that 5E5 preventyed the onset of cognitiver decline but wew wanted to test whether 5E5 would reverse pre-existing impairments. Mice were 10-11 months, an age after cognitive impairment has occured. We used a higher dose of 5E5 in the diet in the reversal study as we felt that this was a more stringent test of our compound. The study design was the same as the earlier prevention study except the animals were 11-12 months and the drug was included at 100 ppm in the diet. All mice learned the platform during the initial acquisition phase and then were randomized into drug-treated or control chow groups. After one month on drug, the mice were tested then retrained on a hidden platform in the second location. All mice membered the first platform position when tested on day 29 but the drug treated mice appeared to find it faster but the difference did not quite make significance (Fig. 3). The drug-treated mice decreased time taken to reach the platform on the second day of training but the control group did not. The mice on the control chow took the same amount of time to find the platform on the second day (day 31) as the first (day 30) showing their inability to learn the platform location.

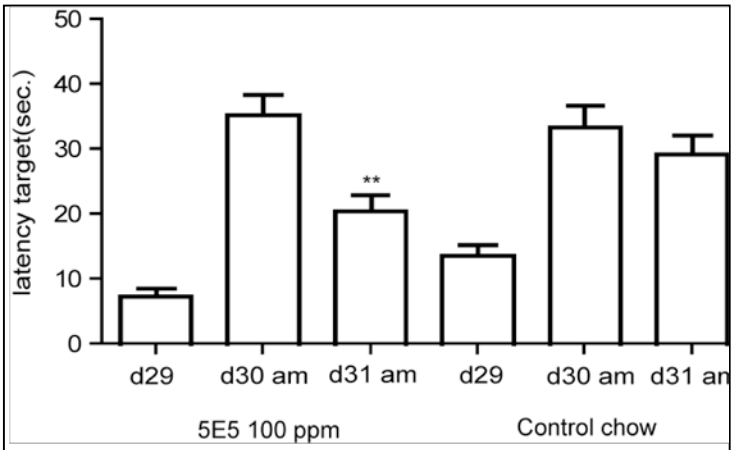

Figure 3. Ability of mice to learn the new position of the hidden platform in a Morris water maze. Mice were fed normal chow or the same diet supplemented with 100 ppm 5E5. Graph shows the latency to find the hidden platform (day 29), which measures retention of a previously learned position, and to learn the new position of the hidden platform (days 30 & 31). Mice are trained on the new location on days 30 and 31. Data were analyzed by ANOVA with Tukey post-hoc analysis.

The drug increased ACHE staining in the CA3 region of the hippocampus consistent with increased cholinergic neuron content (Fig. 4). The mice swam identical distances during the probe test in both studies so the drug did not alter motor activity, and liver enzymes were not altered in either study, although we observed a little reversible steatosis on the 100 ppm diet. The drug did not cause sprouting of DRG peripheral sensory neurons in these mice. Peripheral neurons are labeled for CGRP (Fig. 5). Dark brown indicates cell bodies of CGRP+ve neurons. No sprouting is evident. Overall, our data indicate that treatment with the drug 5E5 improves the ability of NGF+/- mice to learn spatial

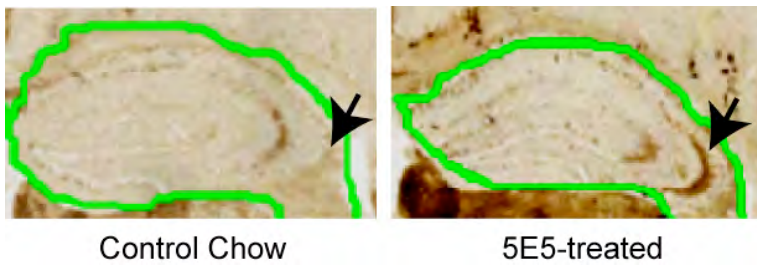

Figure 4. Hippocampal ACHE staining. Arrow points to CA3 region. Green outlines hippocampus. ACHE staining is brown.

information after the onset of cognitive impairments.

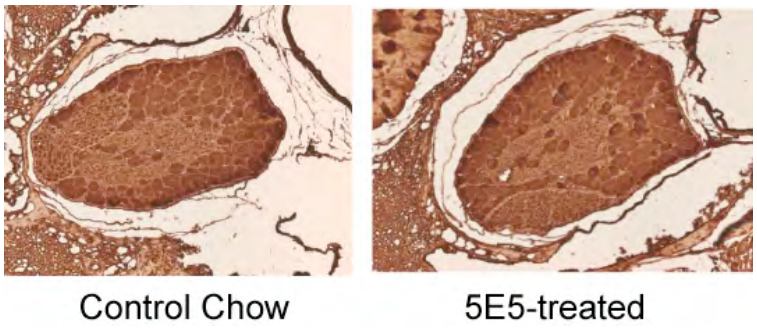

Figure 5. CGRP staining of DRG from control or 5E5-treated mice. Photos show sections through dorsal root ganglia of control or 5E5 treated mice. CGRP +ve neurons are stained dark brown.

Given the ability of 5E5 to improve cognitive function in the NGF+/- neurotrophin deficient model of cognitive declilne, we extended those studies to examine the effect of the drug in a genetic model for Alzheimers Disease the PDAPP mouse. We used PDAPPswind(J20) mice to test our compound 5E5 to see if 5E5 can reverse the pathological changes and memory deficits. These mice express a human APP transgene containing the Swedish (K670/M671L) and Indiana(V717F) mutations. The mice show total Aβ and Aβ1-42 over expression in frontal neocortex and hippocampus. High level of Aβ (1-42) result in age-dependent formation of amyloid plaques in the transgenic mice.

Two studies were performed. The first was a prevention study in young mice before the onset of plaques and the second was a reversal study in older mice after plaques are present. For the prevention study, 24 young 6-month-old PDAPP mice and 4 non-transgenic littermate controls were trained on the Morris water maze. On day one mice were given a pre-screening test with a visible platform to exclude visual or motor problems. Mice were trained on the first platform location on day 2 to day 5. The PDAPP mice were then randomized into two groups. One group received normal chow and the other group received normal chow supplemented with our drug 5E5 at 25 ppm, which was designed to deliver approximately 2.5mg/kg body weight. After one-month treatment, mice were re-tested in the Morris water maze system on the original platform location on day 29 then retrained on a second platform location on days 30 and 31. After a second month on the drug the mice were retested on the second platform location on day 60. Mice were given a probe test on day 29 and 60 after the hidden platform test by removing the platform.

For the reversal study, 24 older 10-month-old PDAPP mice were randomized into two groups. On day one mice were given a pre-screening test with a visible platform to exclude visual or motor problems. One group received normal chow and the other group received normal chow supplemented with our drug 5E5 at 25 ppm for 1 month. Four non-transgenic littermate controls were maintained on normal chow as controls. We verified on independent mice that plaques are detectable at 9 months. The mice were trained on the Morris water maze after 1-month treatment then retested on platform location after a second month on the drug. Mice were trained on the first platform location on day 29 to day 33, then tested for memory retention on day 60. Probe test were performed on days 33 and 60 after the hidden platform test.

Data collection was performed by a computerized video tracking system (SMART, San Diego Instruments). The total swim distance, the average speed, the percentage of swim time spending in the platform quadrant and the latency to find the platform were analyzed. For the prevention study, 5E5-treated mice showed improved learning ability and memory retention. The PDAPP mice showed a profound impairment in both retention, and the ability to learn the second location (Fig. 6). The drug treated mice showed an intermediate phenotype demonstrating a significantly improved ($p<0.05$) ability to learn and retain the location of the second platform (Fig. 6). The 5E5-treated mice also showed an increase in retention of the 2nd platform location on the probe test on Day 60 (Fig. 4, middle panel) and an increase in the

number of entries into quadrant 2 (Fig. 6, right panel). We also observed a significant decrease in latency to first entry into quadrant 2 (data not shown).

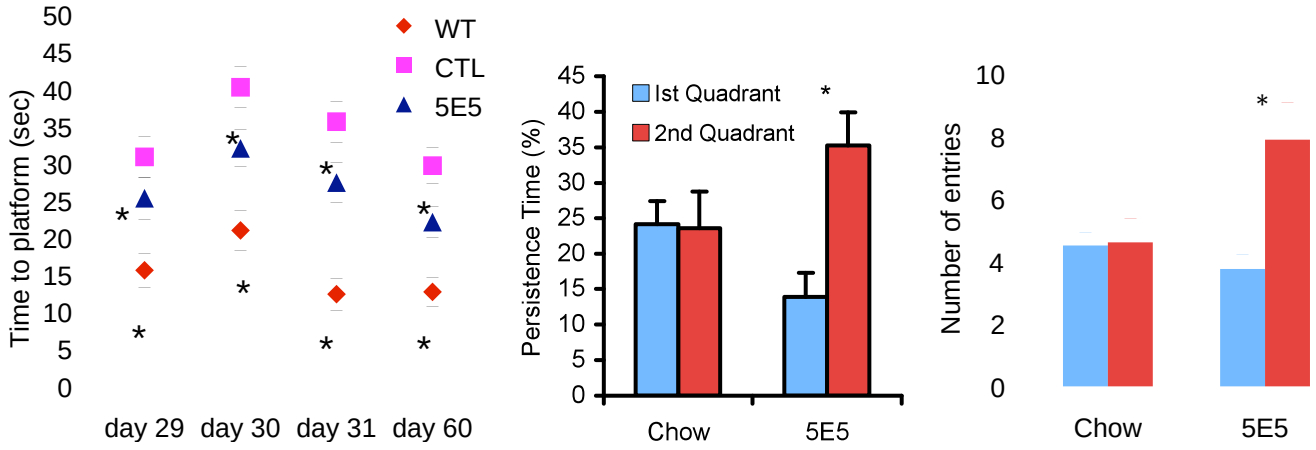

Fig. 6. 5E5 causes an improvement in retention and learning in PDAPP mice. WT indicates non-transgenic littermates. Left panel: Time to platform during hidden platform test. Asterisks indicate significant differences from CTL group. Middle panel: Time spent in quadrants of 1st (red) and 2nd (blue) platform locations during probe test on day 60. Right panel: Number of entries into quadrants 1 and 2 during probe test.

For the reversal study, we observed that learning was significantly enhanced by 5E5 treatment for one month and that retention of the platform location and ability to learn the new location was enhanced (Fig. 7). We also observed that mice retained location of target as well as wild-type non-transgenic mice (Fig. 8). The number of target entries was also normalized by drug treatment (data not shown). During 2 months of treatment, 5E5 didn't cause alter food intake or weight change.

After the behavior test the mice were sacrificed and brain and other tissues were saved for histological analysis of plaque, neuron cell loss and microglia activation. Blood and the liver were also taken for measurement of liver enzymes and histology. Liver enzymes and histology were normal. Brains were sectioned and floating sections stained. Thioflavine S was used to stain amyloid plaques. 5E5-treated mice had reduced plaque number and size in the

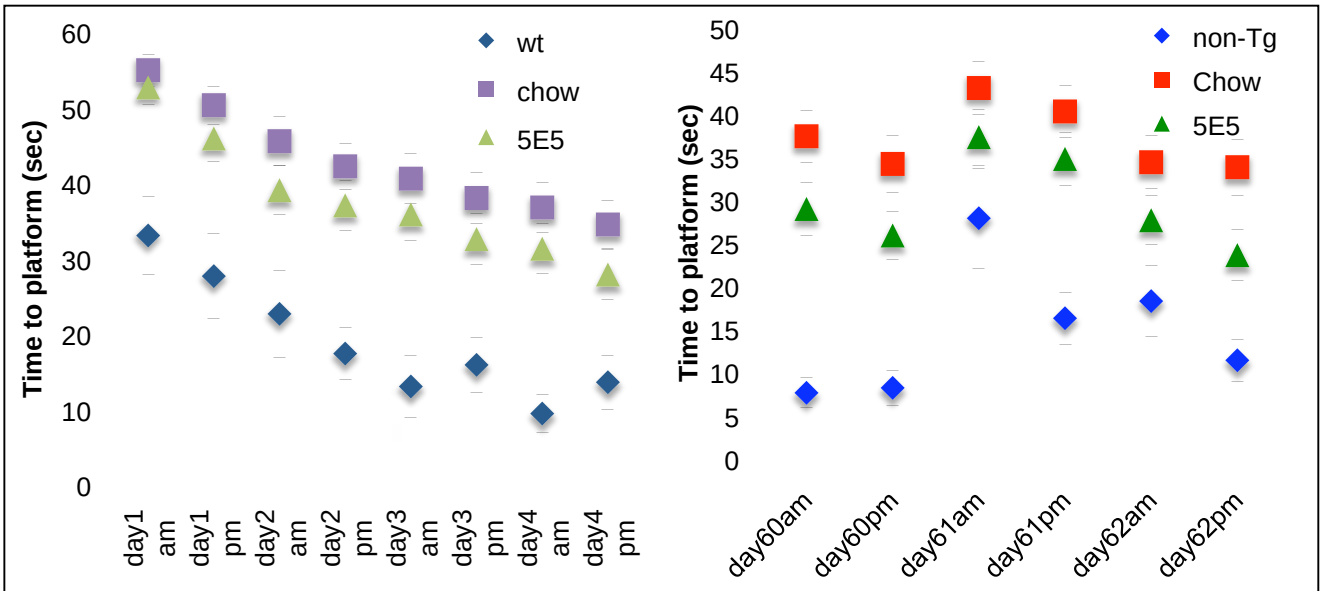

Figure 7: Reversal study. Left panel: Initial learning of hiden platform location. Right panel: retention of platform location and learning of new location on days 60 and 61.

neocortex, cortex and hippocampus. Sections were also stained with Neu-N for neurons and 5E5 reduced neuronal loss in CA3 area of hippocampus. Glial fibrillary Acidic Protein (GFAP) were used to detect activated astrocytes and glia. In nontransgenic mice, no GFAP clusters were detected in neocortex or hippocampus CA1, CA3 and DG. Untreated PDAPP mice showed clusters of GFAP +ve cells and 5E5 reduced GFAP cluster staining in these four area.

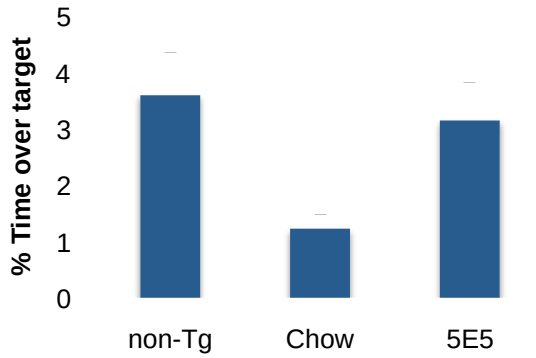

Fig. 8. Time spent over target improved by 5E5

Task 8: *Test selected compounds for neuroprotective effects in a mouse controlled cortical impact (CCI) model of traumatic brain injury.*

The aim of this pilot study was to obtain quantitative characteristics of brain tissue damage such as 1) the size (area) of brain lesion that can be used to perform volume calculation, 2) assessment of BBB damage and 3) the dimension of acute/chronic neuronal cell death using Masson's trichrome stain. After manual annotation of the impact foci, entire ipsi- and contralateral hemispheres, the image analysis tools were fine tuned and employed to perform morphometry of this histochemical staining. To calculate brain lesion volume, the brains were cut into five equally spaced 2 mm coronal slabs with three cross sections placed on the rostral and caudal edges and in the middle of the cortical lesion. The H&E and Masson's trichrome stained sections were digitalized using Aperio scanning system. Using the pen tool, virtual slides were annotated by encircling the lesion edges (penumbra) between intact and pathologically changed brain tissue, and the lesion area (mm2) was reported in annotation window. The rostral-caudal dimensions of the foci were determined through the use of a stereotaxic atlas for the mouse brain, which was viewed electronically side by side with the coronal section images. Distance (mm) between coronal coordinates for bregma +1.54 (rostral position) and -3.88 (caudal position) determined distribution of the lesion volume and was multiplied by the sum of lesion areas (mm2) from all cross sections, yielding the total lesion volume (mm3). The proposed calculation is based on Cavalieri's method that was modified by us for the purpose of volumetric analysis performed on digital slides.

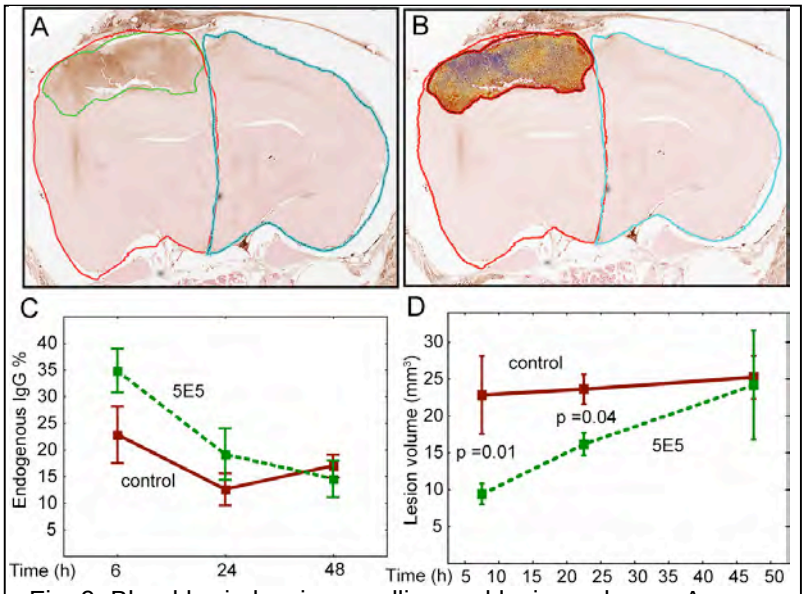

Fig. 9. Blood brain barrier, swelling and lesion volume. A. Staining for endogenous mouse IgG. Lesion outlined in green, contralateral hemisphere in blue. B. Quantification of lesion volume by software algorithm. C. IgG staining as percent of lesion area. D. Lesion volume as a function of time.

We have analyzed the acute morphological changes associated with CCI in mice treated with 5E5. Twenty-six mice were fed the 100 ppm 5E5-containing diet for one week prior to the CCI challenge (5 m/s, 1.2 mm depression) then sacrificed at 6, 24 or 48h. Twenty-four mice were fed control diet. Brains were assessed for lesion volume, blood brain barrier integrity by host IgG staining, and cell death, apoptosis and survival. The whole head paraffin histology method was used to avoid any contact induced artifacts, and sections were stained with Masson's trichrome. The initial lesion volume was reduced in mice treated with 5E5 (Fig. 9). Images are taken on the Aperio Imaging system and analyzed using the ScanScope software using our trained algorithms to analyze the image data and assess the percentage of healthy and injured cells, and the number of dead cells. These algorithms allow the unbiased assessment of post-traumatic changes in the brain and eliminate investigator bias in counting. At 6 hours post-injury both groups developed swelling of the injured hemisphere (ipsilateral to the lesion) and presented blood brain barrier breakdown with extravasation of host IgG indicating that both groups received similar physical injuries (Fig. 9). In contrast, the contralateral hemispheres were negative for swelling and IgG staining. Surprisingly, the contusion volume was significantly smaller in the drug-treated group at 6 and 24 h but was similar to the control mice at 48 h. The contusion volume is determined by both the initial physical impact and the subsequent damage caused by bleeding, the influx of inflammatory cells, and the release of cytokines that cause cell death in the surrounding tissue. It is possible that the drug treatment slows but does not prevent this secondary damage phase. The unbiased counting algorithms were used to assess apoptotic, injured and healthy cells following TUNEL and Masson's trichrome stain morphometry. We found significantly lower number of TUNEL positive cells in the impact focus and the remaining ipsilateral hemisphere in the 5E5-treated mice (Fig. 10). We also observed an increase in surviving neurons and a decrease in injured and necrotic neurons in both the impact focus and ipsilateral hemisphere after 5E5. Drug treatment significantly improved motor function and balance as measured by the number of slips during a beam-walking test (Fig. 11). Leg stretching and open field walking were not impaired by the CCI (data not shown). Mice are currently undergoing cognitive function testing in the Morris water maze as we have performed for the PDAPP and NGF+/- mice.

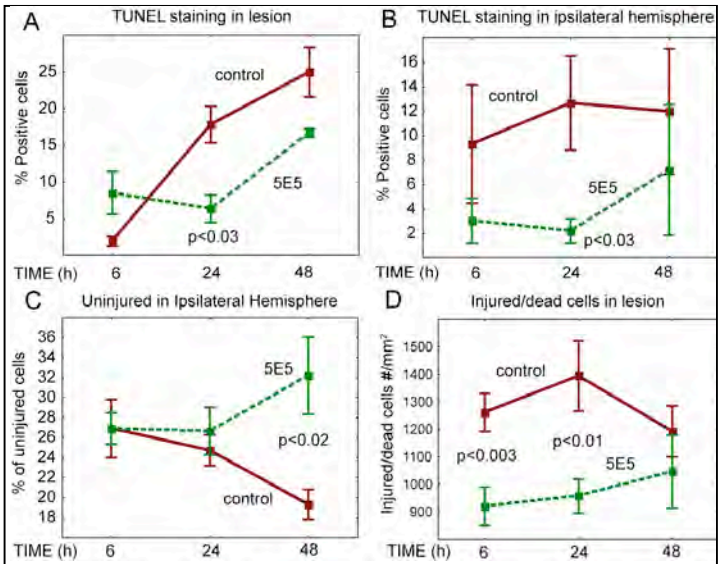

Fig. 10. Quantification of morphometric staining. A: TUNEL positive cells in area of lesion. B: TUNEL positive cells in ipsilateral hemisphere. C: Percent uninjured cells in ipsilateral hemisphere.D: Number of injured/dead cells in area of lesion.

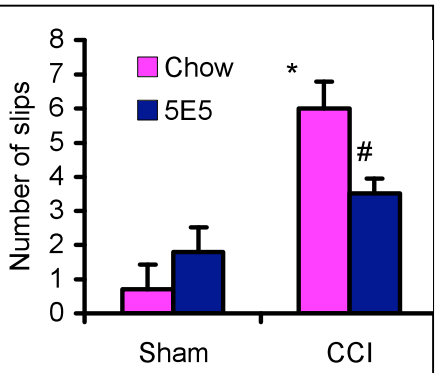

Fig. 11. Number of errors during beam walking test. CCI causes an increase in slips, *p<0.05 vs sham, 5E5 reduces the number of slips after CCI, #p<0.05 vs chow.

Task 9: *Determine pharmacokinetic properties of compounds in mice.*

An aim of our proposal was to obtain preliminary pharmacokinetic data for our drug 5E5 in rodents. We contracted with a PK core at the Burnham Institute to perform a PK analysis in mice. 5E5 was administered at 0.2 mpk by oral gavage. Plasma concentrations were measured by LC/MSMS by the Pharmacology Core at the Burnham Institute. Plasma 5E5 was maximal by 30-60 min (Fig. 12). By 4 h the concentration had fallen to 25% max. The AUC_{0-6} was 4434 ng*hr/mL. The predicted logP value for 5E5 is -0.7 and the compound obeys Lipinski's rules, so the compound should have good bio-availability. The finding of improved learning in the 5E5 treated animals also suggests that the drug must enter the brain.

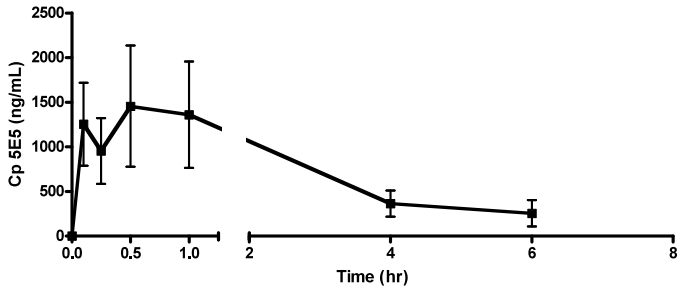

Fig 12: Plasma concentrations of 5E5 following oral

The animal studies required the preparation of a chow by the evaporation of an ethanol solution of 5E5 mixed into the mouse chow. We observed during the PK study that 5E5 itself is metabolized following oral administration and a second stable metabolite is observed by LC. The PK core had difficulty establishing an LC/MSMS assay for 5E5 as it is not stable under the MSMS conditions. Only a very small parent ion peak is observed with pure 5E5 in DMSO but a major peak M^+-28 is observed, which we believe is loss of CO from the molecule under the ionization conditions. It may prove to be the case that 5E5 is a pro-drug form and the actual active agent for neuroprotection is the monohydroxy or even the dihydroxy compound. It is important for us to establish the identity of this species as it may be the true drug that has neuroprotective effects.

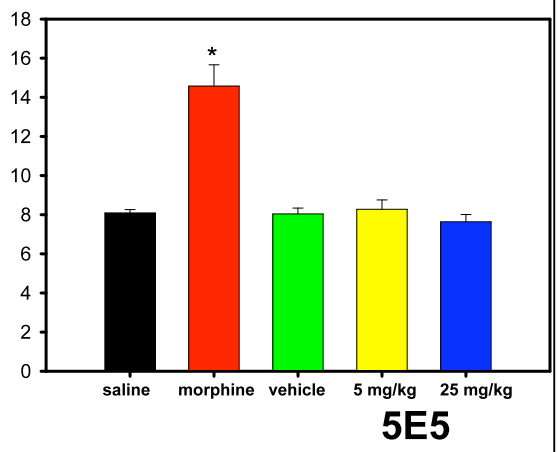

Fig 13. Effect of morphine and 5E5 on latency to lift paw from hot plate.

5E5 was assessed for hyperalgesia as NGF has been shown to cause peripheral sensitization. Mice were tested in a hot plate assay. Dosing with 5E5 did not increase the latency to lift paw from the hot plate indicating that 5E5 does not have an analgesic or hyperalgesic effect (Fig 13).

We also assessed whether 5E% would alter blood clotting using prothrombin and activated partial thromboplastin time assays. 5E5 did not alter clotting time in either assay at concentrations up to 100 µM.

We also investigated the stability of 5E5 in plasma and found that it binds tightly to plasma proteins but not to albumin. Acetic acid extraction is able to liberate >80% of the drug from plasma.

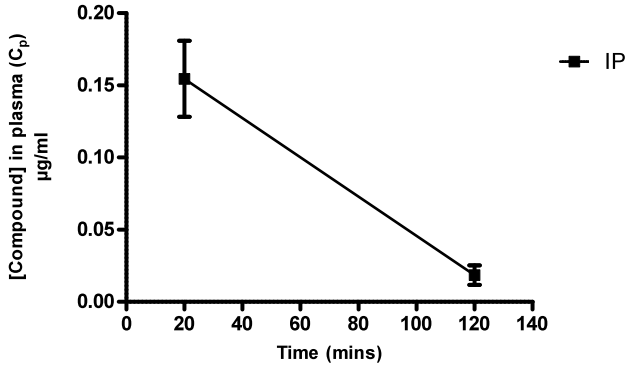

Fig 14. With acid extraction, 5E5 is detectable in plasma following i.p. injection.

With this finding we were able to reassess plasma and brain distribution of the drug. Acid extraction allowed us to measure 5E5 in plasma after i.p. dosing which had not been possible before. Plasma concentration of 5E5 was 0.15 µg/ml at 20 min and declined to 0.02 µg/ml at 120 min (Fig. 14). Interestingly, oral dosing, which had allowed us to see a metabolite peak in the earlier study, did give measurable 5E5 but at ~15% the level of i.p. dosing (data not shown).

We also measured brain concentrations. Following i.p. dosing and acid extraction, the brain concentration of 5E5 was ~10 ng/g brain tissue at 120 min post dosing (data not shown). This data is preliminary but suggests that 5E5 crosses the blood/brain barrier.

Key Research Accomplishments

- Substitution on the 1 and 5 positions are predicted to give good TrkA activation with low IR activation and good survival
- Acid-catalyzed condensation of indoles with dichlorobenzoquinone has prepared a selection of mono-indolyldimethoxybenzoquinones
- The Sonogashira reaction with monoprotected acetylenes can be used to create substituted indoles
- Mathematical modeling of TrkC activation successfully completed
- Demonstrated that 5E5 prevents and reverses cognitive decline in PDAPP mice
- Demonstrated that 5E5 increases neuron survival in PDAPP mice
- Demonstrated that 5E5 does not cause hyperalgesia
- Demonstrated that 5E5 reduces infarct volume in Controlled Cortical Impact model of TBI. Demonstrated that 5E5 reduces apoptosis and increase cell survival following CCI.
- Demonstrated that 5E5 improves motor function after CCI.
- Demonstrated that 5E5 is detectable in blood and brain after i.p. administration.
- Automated slide processing with Digital Pathology Tools allows rapid unbiased assessment of brain injury

Reportable Outcomes

None

Conclusion

The methods developed in this project give us the tools to prepare a large and diverse family of candidate neuroprotective agents. Because these compounds are all small molecules with a relatively modest polar surface area, they should have no difficulty penetrating to the brain, a significant issue with most other drugs (especially neurotrophins) aimed at treating brain injury. Indeed the pharmacokinetic data indicate that the drug is readily absorbed and dispersed following oral administration. The pre-clinical in vivo testing of 5E5 compound showed promising results reducing infarct volume in the controlled coritical impact model of brain injury and in restoring cognitive function in a neurotrophin-deficient model of impaired learning suggesting that it could have potential utility in the treatment of acute traumatic and neurodegenerative diseases. These compounds could lead to a therapeutic for TBI that is easy and economical to manufacture and simple to administer.

References

1. Bo Lin, Michael C. Pirrung, Liu Deng, Zhitao Li, Yufa Liu and Nicholas J.G. Webster. (2007) Neuroprotection by small molecule activators of the NGF receptor. J. Pharmacol. Exp. Ther. 322:59-69. PMID17468299
2. Pirrung, M. C.; Park, K.; Li, Z. Synthesis of 3-indolyl-2,5-dihydroxybenzoquinones. *Org. Lett*. 2001, *2*, 365. Pirrung, M. C.; Deng, L.; Li, Z.; Park, K. Synthesis of 2,5-dihydroxy-3-(indol-3-yl)-benzoquinones by acid-catalyzed condensation. *J. Org. Chem*. 2002, *67*, 8374.
3. Pirrung, M. C.; Wedel, M.; Zhao, Y. 7-Alkyl indole synthesis via a convenient formation/alkylation of lithionitrobenzenes and an improved Bartoli reaction. *Synlett* 2002, 143.
4. Bermpohl D, You Z, Korsmeyer SJ, Moskowitz MA, Whalen MJ (2006) Traumatic brain injury in mice deficient in Bid: effects on histopathology and functional outcome. J Cereb Blood Flow Metab 26:625-633.
5. Krajewska M, Smith LH, Rong J, Huang X, Hyer ML, Zeps N, Iacopetta B, Linke SP, Olson AH, Reed JC, Krajewski S (2009). Image Analysis Algorithms for Immunohistochemical Assessment of Cell Death Events and Fibrosis in Tissue Sections. J Histochem Cytochem 2009 Mar 16. [Epub ahead of print]

Appendices

None